Mineralogical Magazine, October 2013, Vol. 77(7), pp. 3039–3046

Barikaite, $Pb_{10}Ag_3(Sb_8As_{11})_{\Sigma 19}S_{40}$, a new member of the sartorite homologous series

D. Topa[1,*], E. Makovicky[2], H. Tajedin[3], H. Putz[4] and G. Zagler[4]

[1] Natural History Museum Vienna, Burgring 7, A-1010 Vienna, Austria
[2] Department of Geoscience and Resource Management, University of Copenhagen, Østervoldgade 10, DK-1350, Copenhagen K, Denmark
[3] Department of Geology, Faculty of Basic Sciences, Tarbiat Modares University, P.O. Box 14115-175, Tehran, Iran
[4] Department of Material Engineering and Physics, University of Salzburg, Hellbrunnerstraβe 34, A-5020 Salzburg, Austria

[*Received 28 June 2013; Accepted 7 October 2013; Associate Editor: A. Pring*]

ABSTRACT

Barikaite, ideally $Pb_{10}Ag_3(Sb_8As_{11})_{\Sigma 19}S_{40}$, is a new mineral species from the Barika Au-Ag deposit, Azarbaijan Province, western Iran. It was formed in fractures developed in silica bands situated in massive banded pyrite and baryte ores. These fractures house veinlets that contain a number of Ag-As-Sb-Pb-rich sulfosalts, tetrahedrite-tennantite, realgar, pyrite and electrum. Barikaite appears as inclusions in guettardite. The mineral is opaque, greyish black with a metallic lustre; it is brittle without any discernible cleavage. In reflected light barikaite is greyish white, pleochroism is distinct, white to dark grey. Internal reflections are absent. In crossed polars, anisotropism is distinct with rotation tints in shades of grey. The reflectance data (%, in air) are: 37.0, 39.3 at 470 nm, 34.1, 36.9 at 546 nm, 33.1, 36.2 at 589 nm and 31.3, 34.1 at 650 nm. The Mohs hardness is 3−3½, microhardness VHN_{50} exhibits the range 192−212, with a mean value of 200 kg mm^{-2}. The average results of five electron-microprobe analyses in a grain are (in wt.%): Pb 35.77(33), Ag 5.8(1), Tl 0.15(08), Sb 18.33(09), As 15.64(16), S 24.00(15), total 99.69(10) wt.%, corresponding to $Pb_{9.31}Ag_{2.90}Tl_{0.04}(Sb_{8.12}As_{11.26})_{\Sigma 19.36}S_{40.37}$ (on the basis of 32Me + 40S = 72 a.p.f.u.). The simplified formula, $Pb_{10}Ag_3(Sb_8As_{11})_{\Sigma 19}S_{40}$, is in accordance with the results of a crystal-structure analysis, and requires Pb 37.89, Ag 5.91, Sb 17.79, As 15.05 and S 23.42 (wt.%). The variation of chemical composition is minor, the empirical formula ranging from $Pb_{10.39}Ag_{2.32}Tl_{0.02}Sb_{7.52}As_{11.27}S_{40.49}$ to $Pb_{9.24}Ag_{2.93}Tl_{0.04}Sb_{8.13}As_{11.35}S_{40.31}$. Barikaite has monoclinic symmetry, space group $P2_1/n$ and unit-cell parameters a 8.5325(7) Å, b 8.0749(7) Å, c 24.828(2) Å, and β 99.077(6)°, $Z = 1$. Calculated density for the empirical formula is 5.34 (g cm^{-3}). The strongest eight lines in the (calculated) powder-diffraction pattern [d in Å(I)(hkl)] are: 3.835(63)(022), 3.646(100)(016), 3.441(60)(212), 3.408(62)($\bar{2}$14), 2.972(66)($\bar{2}$16), 2.769(91)(222), 2.752(78)($\bar{4}$24) and 2.133(54)(402). Barikaite is the N = 4 member of the sartorite homologous series with a near-equal role of As and Sb, which have an ordered distribution pattern in the structure. It is a close homeotype of rathite and more distantly related to dufrénoysite (both distinct, pure arsenian N = 4 members) and it completes the spectrum of Sb-rich members of the sartorite homologous series. The new mineral and its name have been approved by the IMA-CNMNC (IMA 2012-055).

Keywords: barikaite, sulfosalt, new mineral, sartorite homologous series, Barika deposit, Iran.

Introduction and previous investigations

The originally described members of the sartorite homologous series defined by Makovicky (1985) were arsenic-based species. After the period of

* E-mail: dan.topa@nhm-wien.ac.at
DOI: 10.1180/minmag.2013.077.7.13

classical morphological studies on these minerals, the X-ray diffraction (XRD) studies and crystal structure determinations by Le Bihan (1962) and especially by Nowacki's group (Iitaka and Nowacki, 1961; Engel and Nowacki, 1969, 1970; Ribár *et al*., 1969; Marumo and Nowacki, 1965, 1967; Ozawa and Nowacki, 1974) led to a final clarification of their complex crystallography and mineralogy. Jambor (1967*a*,*b*) was perhaps the first mineralogist who described antimony-containing analogues of the arsenian phases of the sartorite homologous series, based on the material from Madoc, Ontario, Canada. Later, Mantienne (1974) and Johan and Mantienne (2000) described the Alpine locality of Jas Roux as another important source of Sb-As sulfosalts, second only to the classical locality of Madoc. Other occurrences found in literature, e.g. Pitone marble quarry, Seravezza, Tuscany (Bracci *et al*., 1980) and Silverton, Colorado (www.mindat.org), Zarshouran, NW Iran (Paar *et al*., 2009), and Săcărimb, Romania (Ciobanu *et al*., 2005), do not seem to reach the abundance and diversity of these two localities. The discovery of a new locality of As-Sb sulfosalts, at Barika in the Azarbaijan Province of western Iran (Khodaparast *et al*., 2010), enabled us to contribute a new member to the spectrum of known As-Sb members of the sartorite homologous series. The description of the new member, barikaite, is the topic of this contribution. The name of the mineral is for the type locality. The mineral and its name have been approved by the CNMNC–IMA, under the number IMA 2012–055 (Topa *et al*., 2013*a*). The holotype specimen of barikaite is deposited in the mineral collection of the Natural History Museum Vienna, Austria, with specimen number N 9581.

Provenance

The Barika ore deposit is a gold-rich volcanogenic massive sulfide deposit of Cretaceous age. It is situated in the metamorphic Sanandaj-Sirjan Zone that stretches as a NW–SE zone in the province of Western Azarbaijan (western Iran). Greenschist metamorphism and deformation in the form of shear zones overprinted the original synvolcanic stratiform textures. Metamorphism produced a granoblastic texture of pyrite, and ductile deformation resulted in folding, recrystallization and boudinage.

The lens-like deposit, ~150 m long and up to 20 m thick, consists of massive to semi-massive banded pyrite and baryte ores accompanied by locally developed silica bands (Khodaparast *et al*., 2010). Pyrite, sphalerite, galena, tetrahedrite-tennantite and stibnite were deposited during the synvolcanogenic hydrothermal activity. Brittle deformation, fractured porphyroblasts of pyrite and especially the silica bands modified the original situation. Fractures host veinlets that contain a number of Ag-As-Sb-Pb-rich sulfosalts: tetrahedrite-tennantite, stephanite, pyrargyrite, trechmannite, smithite, miargyrite, andorite, geocronite, seligmannite, guettardite (Makovicky *et al*., 2012), and in addition, realgar, pyrite and Au-Ag alloys. The chemical remobilization of the components originally housed by the stratiform ores, which led to the formation of these minerals, took place at the margins of the orebody. It produced economically important concentrations of recoverable gold in the form of Au-Ag alloys.

The specimen that yielded barikaite is a portion of a quartz vein hosting irregular thin veinlets and nests of sulfosalts in a mass of quartz and baryte. Barikaite appears to be rare and it was always found in association with guettardite. Figure 1 shows that barikaite is being replaced by guettardite from the margins, resulting in corroded crystals (Fig. 1*a*,*b*) or in disjointed and strongly corroded remnants of what obviously was a solid barikaite aggregate (Fig. 1*c*). Optical investigation shows that most of the guettardite in Fig. 1*b* displays twinning in contrast to barikaite, in which no twinning was observed. As well as barikaite, a Zn-Hg-bearing tennantite, smithite, Sb-bearing smithite and guettardite were detected, together with two new mineral species, (IMA 2012-062 and IMA 2012-087) presented in Fig. 1*d* (Topa *et al*., 2013*b*,*c*), which will be described elsewhere.

Appearance and physical properties

Barikaite occurs as anhedral grains and no crystal forms are present. Twinning was not observed. In hand specimen, it is greyish black, opaque with metallic lustre. The streak is dark grey. Indentation hardness VHN_{50} is 189–208 kg mm^{-2}, yielding a mean value of 200 kg mm^{-2}. Barikaite is brittle with irregular fracture; no cleavage or parting has been observed. The experimental density could not be measured because of a paucity of available material and admixture with guettardite. The calculated density, based on the empirical formula, is 5.34 g cm^{-3}.

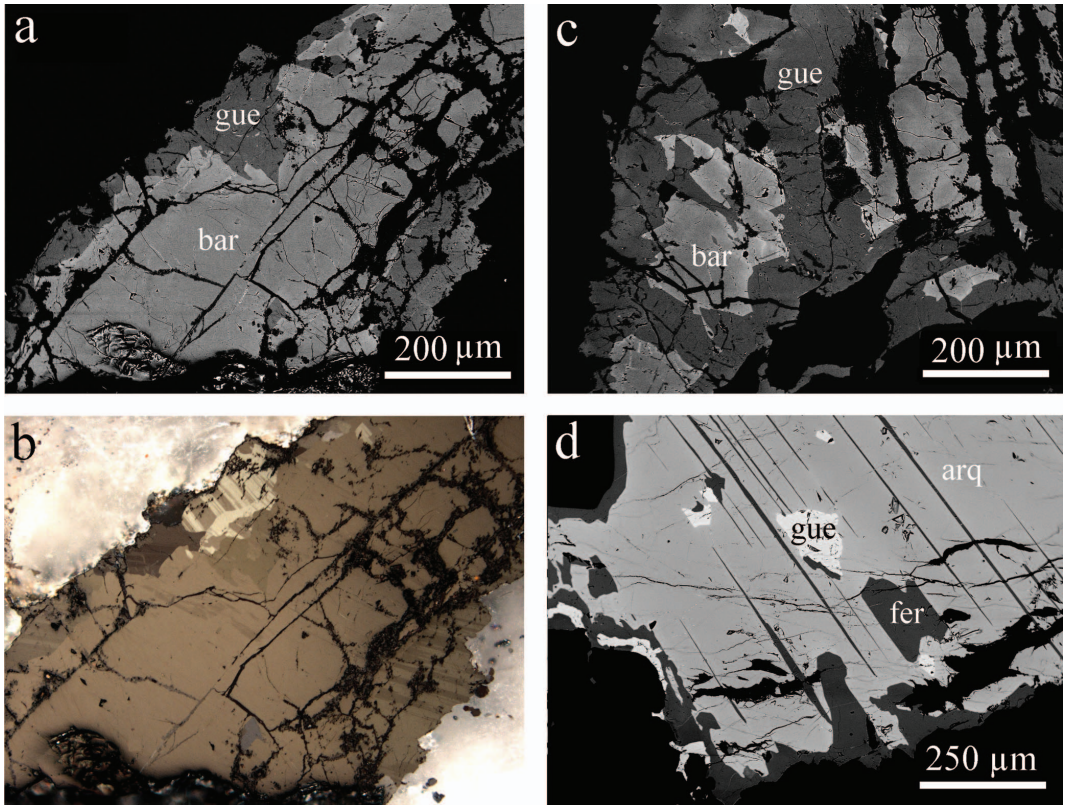

FIG. 1. (*a*) Elongated crystal of barikaite (bar, light grey) replaced from the margins by guettardite (gue, dark). (*b*) In reflected light guettardite is twinned. (*c*) Disjointed and strongly corroded remnants of an originally solid barikaite aggregate strongly replaced by guettardite. Lighter portions (margins and replacement remnants) represent barikaite with a smaller substitution percentage. (*d*) A very common assemblage of arsenquatrandorite (arq) guettardite (gue) and ferdowsiite (fer).

Optical properties

In polarized reflected light, barikaite is greyish white, with distinct bireflectance in grey tones, visible especially in oil immersion. Anisotropy under crossed polars is distinct, in shades of grey. Internal reflections were not observed. Reflectance data were obtained in air using a Leitz MPV-SP microscope photometer and a WTiC standard (Table 1). The measured reflectance values decrease by ~7% from $\lambda = 400$ nm to $\lambda = 700$ nm. ΔR observed in the available material is only 2–3%.

TABLE 1. Refectance data (in air) for barikaite.

λ (nm)	R_{min}	R_{max}	λ (nm)	R_{min}	R_{max}
400	34.5	38.1	560	34.0	36.6
420	37.1	39.6	580	33.3	36.4
440	37.7	39.8	**589**	**33.1**	**36.2**
460	37.4	39.8	600	32.8	35.9
470	**37.0**	**39.3**	620	32.0	35.2
480	36.7	39.2	640	31.5	34.4
500	35.7	38.2	**650**	**31.3**	**34.1**
520	34.9	37.3	660	31.3	34.0
540	34.2	37.0	680	30.7	33.8
546	**34.1**	**36.9**	700	30.3	33.3

Chemical composition

Barikaite and the associated sulfosalts minerals were analysed using a JEOL Superprobe JXA-8600 electron microprobe, controlled by the *Probe*

for Windows system of programs, and operated at 25 kV and 20 nA, with a beam diameter of 5 μm. Wavelength-dispersion data were collected using the following standards and emission lines: Bi_2S_3 (Bi*L*α), galena (Pb*M*α), chalcopyrite (Cu*K*α, Fe*K*α), Ag metal (Ag*L*α), Sb_2S_3 (Sb*L*α, S*K*α), lorandite (Tl*L*α) and InAs (As*L*α). The raw data were corrected with the on-line ZAF-4 procedure. The results of the electron-microprobe analyses are compiled in Table 2. Iron, copper and bismuth are absent from barikaite, below the detection limits of 0.04, 0.03 and 0.15 wt.%, respectively. Chemical compositions of associated sulfosalt minerals are given in Table 2 as well. The empirical formula for barikaite (Table 2), ideally based on 32Me + 40S a.p.f.u. (where Me indicates cations), in agreement with the results of structure determination, is: $Pb_{9.31}Ag_{2.90}Tl_{0.04}$ $As_{11.26}Sb_{8.12}S_{40.37}$ and the simplified formula is $Pb_{10}Ag_3(Sb_8As_{11})_{\Sigma 19}S_{40}$.

The sartorite homologous series was described in detail by Makovicky (1985) in terms of general formula, definition of the order number (N) of the homologue and substitution mechanisms of Ag/Tl and As/Sb for Pb. Dufrénoysite and rathite are members of the sartorite homologous series with homologue number N = 4. Rathite has been reinvestigated structurally and chemically by Berlepsch *et al*. (2002). They showed that the complex composition of rathite, $Pb_8Pb_{4-x}(Tl_2As_2)_x(Ag_2As_2)As_{16}S_{40}$ and structure with space group $P2_1/c$, is a result of two independent heterovalent substitutions $Ag^+ + As^{3+}$ for $2Pb^{2+}$ and $Tl^+ + As^{3+}$ for $2Pb^{2+}$ which modified dufrénoysite, $Pb_{16}As_{16}S_{40}$ with reduced symmetry $P2_1$, both chemically and structurally. They stated also that Ag substitution is essential for the formation of rathite, that the Tl substitution can be optional and that minor Sb^{3+} may replace As^{3+}. The Tl-free rathite will have the simplified formula: $Pb_{12}Ag_2As_{18}S_{40}$, where 4Pb were replaced by 2Ag and 2As, with respect to dufrénoysite. A comparison with the barikaite simplified formula, $Pb_{10}Ag_3(As_{11}Sb_8)_{\Sigma 19}S_{40}$, shows that Ag substitution in barikaite is one third stronger than in rathite, in comparison to dufrénoysite, with 6Pb replaced by 3Ag and 3As. Moreover, in barikaite a 42% Sb replacement of As is observed, in comparison with rathite and dufrénoysite.

A small substitution range was observed for barikaite (Table 3): the limiting compositions in atomic contents p.f.u. are $Pb_{10.39}Ag_{2.32}Tl_{0.02}$ $Sb_{7.52}As_{11.27}S_{40.49}$ (empirical homologue order N = 3.83, 63.4% [Ag+(As,Sb)] substitution for 2Pb; see below) and $Pb_{9.24}Ag_{2.93}Tl_{0.04}$ $Sb_{8.13}As_{11.35}S_{40.31}$ with N = 3.84 and 80.4% [Ag+(As,Sb)] substitution for 2Pb, so that the composition range is ~17% substitution. The majority of barikaite analyses, however, remain in the substitution range 76.7–80.4% (Table 3); the less substituted areas, with substitution percentages of 63.4–67.9 represent marginal portions of the aggregates, which are close to, and partly separated by, the replacing guettardite (Fig. 1*c*).

The substitution percentage describes a position of the phase on a theoretical substitution line N = 4, between the ideal compositions $Pb_{16}As_{16}S_{40}$ and $Pb_8Ag_4(As,Sb)_{20}S_{40}$. The latter composition has all substitutable Pb sites 100% substituted, with 2Pb exchanged by Ag + (As,Sb). The additional substitution of 2Pb by Tl + (As,Sb) is negligible in barikaite. The empirical homologue order N is based on a general calculation

TABLE 2. Average results of electron-microprobe analyses.

Mineral*	NA	Ag	Cu	Pb	Sb	As	S	Total
Barikaite§	5	5.80(10)	–	35.77(33)	18.33(09)	15.64(16)	24.00(15)	99.69(10)
IMA 2012-62	10	38.81(70)		0.76(08)	26.06(81)	10.64(70)	23.21(13)	99.59(82)
IMA 2012-87	6	11.83(23)	1.44(10)	20.42(26)	35.57(35)	6.59(36)	23.67(17)	99.52(36)
Guettardite	11	–	–	37.63(17)	22.78(74)	14.97(21)	24.36(17)	99.74(84)
Smithite	6	41.97(16)	–	–	13.96(18)	19.47(18)	24.51(18)	99.91(36)

* Shown in Fig. 1*a*, *c* and *d* (except smithite), ferdowsiite (IMA 2012-62) and arsenquatrandorite (IMA 2012-87). NA: number of point analyses; compositions are reported in wt.%.
§ contains 0.15(08)% Tl, calculated chemical homologue number is N = 3.85 (Makovicky, 1985).
The empirical formula for barikaite (based on 72 a.p.f.u., 32Me+40S) is $Pb_{9.31}Ag_{2.90}Tl_{0.04}As_{11.26}Sb_{8.12}S_{40.37}$.
The simplified formula is $Pb_{10}Ag_3(Sb_8As_{11})S_{40}$.

TABLE 3. Chemical variations for barikaite.

No	Zone	NA	Ag	Pb	Tl	Sb	As	S	Total	N	Ag%	Tl%
1	Fig. 1*a* core	5	5.51(07)	36.18(35)	0.13(07)	18.36(14)	15.52(13)	23.92(15)	99.62(13)	3.82	76.7	0.9
2	Fig. 1*a* rim	6	5.87(07)	35.50(20)	0.13(07)	18.37(12)	15.77(13)	23.98(159	99.63(20)	3.84	80.4	0.9
3	Fig. 1*c* incl.	6	4.55(09)	39.21(42)	0.07(05)	16.68(44)	15.38(29)	23.65(08)	99.55(42)	3.83	63.4	0.5
4	Fig. 1*c* incl.	6	4.93(10)	38.19(22)	0.22(03)	17.49(21)	15.18(09)	23.66(10)	99.68(14)	3.86	67.9	1.5

1 $Ag_{2.77}Tl_{0.04}Pb_{9.45}As_{11.21}Sb_{8.16}S_{40.38}$
2 $Ag_{2.93}Tl_{0.04}Pb_{9.24}As_{11.35}Sb_{8.13}S_{40.31}$
3 $Ag_{2.32}Tl_{0.02}Pb_{10.39}As_{11.27}Sb_{7.52}S_{40.49}$
4 $Ag_{2.50}Tl_{0.06}Pb_{10.09}As_{11.09}Sb_{7.87}S_{40.39}$

NA: number of point analyses; compositions are reported in wt.%.
Calculated chemical homologue number (N) after Makovicky (1985).
The empirical formulae for barikaite is based on 72 a.p.f.u., 32Me+40S.
Ag% and Tl% are values of [Ag+(As,Sb)] and [Tl+(As,Sb)] substitution for 2Pb.

scheme for the homologue order N of the sartorite homologues (Makovicky, 1985). The empirical N values derived from the chemical analyses are in fair agreement with the crystallographic value of N = 4.

Single-crystal and crystal-structure data

A Bruker AXS three-circle diffractometer equipped with a CCD area detector system (University of Salzburg) was used to perform the single-crystal study on a fragment of barikaite extracted mechanically from the chemically and optically analysed polished section. Barikaite is monoclinic with space group $P2_1/n$: unit-cell parameters refined from single-crystal data are as follows: *a* 8.5325(7) Å, *b* 8.0749(7) Å, *c* 24.828(2) Å, and β 99.077(6)°. The resulting unit-cell volume is 1688.8(10) Å^3; Z = 1 for the formula $Pb_{10}Ag_3(Sb_8As_{11})_{\Sigma 19}S_{40}$. Powder diffraction data could not be obtained because of the paucity and intimate intergrowth nature of the material investigated. A theoretical powder pattern, calculated using the *PowderCell 2.3* program (Kraus and Nolze, 1999) and crystallographic and structural data obtained by our single-crystal study and crystal-structure determination, is reproduced in Table 4. Experimental details of the crystal-structure determination on barikaite and a detailed discussion are given in a parallel paper (Makovicky and Topa, in press).

The crystal structure of barikaite is a typical structure of a member of the sartorite homologous series (Makovicky, 1985; Berlepsch *et al*., 2001, 2002, 2003; Ferraris *et al*., 2008). It contains (001) zig-zag walls composed of tricapped trigonal coordination prisms around Pb atoms, which separate structure slabs composed primarily of coordination polyhedra around As and Sb atoms, interspersed with lesser amounts of Ag and Pb atoms. Because of pronounced lone-electron pair activity of the As and Sb atoms, these slabs consist of tightly bonded double-layers formed by coordination pyramids of AsS_5 and SbS_5, and separated by interspaces left for accommodation of the lone electron pairs. As can be seen in Fig. 2, every double-layer, with the PbS_9 polyhedron attached to its side, spans four coordination polyhedra of cations. Thus, barikaite is the N = 4 member of the sartorite homologous series and belongs to its As-Sb sub-series, with both metalloids present in substantial amounts, unlike rathite and dufrénoysite, which are the arsenic-based N = 4 members.

TABLE 4. Calculated X-ray powder-diffraction data for barikaite.

I_{rel}	d_{calc} (Å)	h	k	l	I_{rel}	d_{calc} (Å)	h	k	l	I_{rel}	d_{calc} (Å)	h	k	l
19	6.74	0	1	2	12	2.908	$\bar{2}$	2	2	**54**	**2.133**	$\bar{\mathbf{4}}$	**0**	**2**
11	5.74	0	1	3	41	2.872	0	2	6	5	2.096	0	2	10
4	5.50	$\bar{1}$	1	2	7	2.867	1	1	7	5	2.071	2	3	4
9	5.45	1	0	3	33	2.865	0	1	8	6	2.059	$\bar{2}$	3	6
13	4.88	0	1	4	13	2.858	2	2	1	3	2.044	$\bar{2}$	1	11
30	4.21	2	0	0	14	2.846	$\bar{2}$	2	3	13	2.022	0	3	8
13	4.19	$\bar{2}$	0	2	9	2.7892	2	1	5	4	2.006	2	2	8
13	4.19	0	1	5	**91**	**2.769**	**2**	**2**	**2**	9	1.992	0	4	2
28	4.04	0	2	0	12	2.754	$\bar{2}$	1	7	3	1.986	$\bar{2}$	2	10
14	3.974	1	0	5	**78**	**2.752**	$\bar{\mathbf{2}}$	**2**	**4**	4	1.972	1	2	10
63	**3.835**	**0**	**2**	**2**	7	2.676	$\bar{3}$	1	2	4	1.963	4	1	2
10	3.804	2	0	2	10	2.676	0	3	1	4	1.960	0	4	3
5	3.760	$\bar{2}$	0	4	17	2.655	2	2	3	10	1.915	2	3	6
100	**3.646**	**0**	**1**	**6**	12	2.646	0	2	7	8	1.915	0	3	9
9	3.641	1	2	0	9	2.641	$\bar{3}$	1	3	11	1.902	$\bar{2}$	3	8
9	3.620	0	2	3	10	2.635	$\bar{2}$	2	5	6	1.888	3	3	2
23	3.618	2	1	1	10	2.629	0	3	2	4	1.886	$\bar{4}$	2	2
25	3.592	$\bar{2}$	1	3	9	2.465	0	3	4	4	1.868	4	2	0
60	**3.441**	**2**	**1**	**2**	8	2.346	0	1	10	8	1.861	$\bar{4}$	2	4
62	**3.408**	$\bar{\mathbf{2}}$	**1**	**4**	7	2.318	$\bar{1}$	3	5	12	1.851	4	1	4
8	3.372	0	2	4	41	2.311	2	0	8	3	1.846	3	3	3
4	3.241	2	0	4	37	2.281	$\bar{2}$	0	10	6	1.834	2	3	7
12	3.231	2	1	3	11	2.268	2	3	0	9	1.831	$\bar{4}$	1	8
3	3.196	$\bar{2}$	0	6	11	2.265	$\bar{2}$	3	2	10	1.823	0	2	12
11	3.194	$\bar{2}$	1	5	4	2.258	0	2	9	8	1.821	$\bar{2}$	3	9
52	3.117	0	2	5	18	2.248	0	3	6	8	1.821	2	4	0
24	3.065	0	0	8	11	2.222	2	1	8	10	1.819	$\bar{2}$	4	2
43	3.008	2	1	4	3	2.197	2	3	2	5	1.806	2	4	1
66	**2.972**	$\bar{\mathbf{2}}$	**1**	**6**	10	2.195	$\bar{2}$	1	10	4	1.806	2	1	11
13	2.932	$\bar{2}$	2	1	4	2.189	$\bar{2}$	3	4	9	1.803	$\bar{2}$	4	3
14	2.915	2	2	0	4	2.149	0	1	11	4	1.797	3	3	4

The theoretical pattern was calculated using *PowderCell 2.3* (Kraus and Nolze, 1999) in Debye-Scherrer configuration employing Cu$K\alpha$ radiation (λ = 1.540598 Å), fixed slit, no anomalous dispersion, for I_{rel} > 2.99. Cell parameters, space group, atom positions, site occupancy factors and isotropic displacement factors from the crystal structure determination were used (Makovicky and Topa, in press).

The predominantly As-occupied and Sb-occupied coordination polyhedra in the slabs are distributed in a chess-board pattern, similar to those observed in the N = 3 members, guettardite (Makovicky *et al.*, 2012) and twinnite (Makovicky and Topa, 2012). This distribution contributes to the characteristic 8.52 Å *a* parameter of the unit cell and represents a feature which separates it from rathite. In addition to two prismatically coordinated Pb sites, one As and one Sb site, the crystal structure contains two mixed As-Sb coordination polyhedra with different element proportions, one Ag-As polyhedron, and one complicated mixed Pb-Sb-Ag site. A detailed description of the crystal structure is given by Makovicky and Topa (in press).

Related species

Barikaite is a homeotype of the pure arsenian N = 4 member of the sartorite homologous series, rathite, first structurally characterized as 'rathite I' by Marumo and Nowacki (1965) and later in a detailed study by Berlepsch *et al.* (2002). According to Makovicky (1985), 'rathite I' of Le Bihan (1962) might have been dufrénoysite and not rathite. The unit cell of rathite in the same $P2_1/n$ setting as the present barikaite cell is

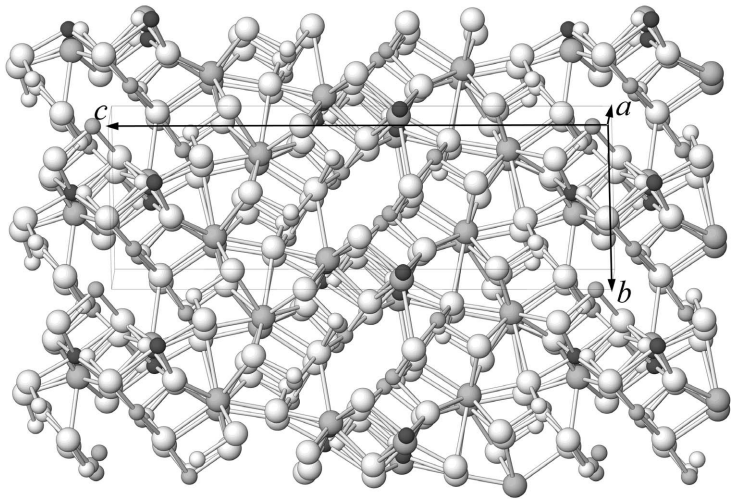

FIG. 2. Crystal structure of barikaite in oblique projection on (100). Large white spheres: S; medium large, light grey spheres: Pb; small light grey and white spheres: Sb and As, respectively; small black spheres: Ag. The unit cell is outlined.

a 8.496(1) Å, *b* 7.969(1) Å, *c* 24.980(3) Å and β 98.918(2)° (Berlepsch *et al*., 2002). A slight increase in the *a* and *b* parameters of barikaite (above) *vs*. those in rathite is caused by the large amount of Sb in barikaite. This comparison confirms the structural similarity of the two minerals; the presence of As–Sb ordering in barikaite does not change the space group but it separates barikaite from rathite. Type barikaite has a higher degree of Ag + (As,Sb) substitution for 2 Pb than rathite, $Pb_{12}As_{18}Ag_2S_{40}$, studied by Berlepsch *et al*. (2002), in which Sb represents only 5% of the metalloids. Typical of barikaite is a metalloid site with strong affinity for Sb, which is fully occupied by this element (Makovicky and Topa, in press).

Dufrénoysite, $Pb_{16}As_{16}S_{40}$, with *a* 7.90(1), *b* 25.74(5), *c* 8.37(4), β 90.35(15)°, space group $P2_1$, is a more distant homeotype of barikaite, with a markedly different monoclinic β angle. It lacks substitution by silver and, with the absence of inversion centres, the two surfaces of tightly-bonded double-layers have different occupancies by cations (Ribár *et al*., 1969). In barikaite these layers are related by inversion. Both layers also exhibit higher occupancy by Pb in dufrénoysite than in barikaite and rathite. Veenite (Jambor, 1967*a*,*b*) is the As-Sb analogue of dufrénoysite.

Guettardite and twinnite, with crystal structures and OD relationships described by Makovicky *et al*. (2012) and Makovicky and Topa (2012), are the As-Sb based N = 3 members of the same sartorite homologous series as barikaite, with sartorite being their arsenian homeotype. Baumhauerite (Engel and Nowacki, 1969) and its Sb-As homeotype, boscardinite (Orlandi *et al*., 2012) are the combinatorial N = 3,4 homologues with the N = 3 and N = 4 slabs alternating in a regular sequence. Recognition of all these phases from the results of electron microprobe analyses is based on calculation formulae for the N values, given by Makovicky (1985).

Barikaite is the last of the missing As-Sb analogues of the known As-based sartorite homologues, completing the spectrum of ordered As-Sb derivatives.

Acknowledgements

The authors gratefully acknowledge the financial support of the Research Council for the Nature and Universe, Denmark (grant no. 272-08-0227). The manuscript benefited from the helpful comments of Herta Effenberger and an anonymous referee, and from the editorial care of Peter Williams.

References

Berlepsch, P., Makovicky, E. and Balić-Žunić, T. (2001) Crystal chemistry of sartorite homologues and related sulfosalts. *Neues Jahrbuch für Mineralogie Abhandlungen*, **176**, 45–66.

Berlepsch, P., Armbruster, T. and Topa, D. (2002) Structural and chemical variations in rathite, $Pb_8Pb_{4-x}(Tl_2As_2)_x(Ag_2As_2)As_{16}S_{40}$: modulations of a parent structure. *Zeitschrift für Kristallographie*, **217**, 1–10.

Berlepsch, P., Armbruster, T., Makovicky, E. and Topa, D. (2003) Another step toward understanding the true nature of sartorite: Determination and refinement of a nine-fold superstructure. *American Mineralogist*, **88**, 450-461.

Bracci, G., Dalena, D., Orlandi, P., Duchi, G. and Vezzalini, G. (1980) Guettardite from Tuscany, Italy: A second occurrence. *The Canadian Mineralogist*, **18**, 13–15.

Ciobanu, C.L., Cook, N.J., Capraru, N., Damina, G. and Cristea, P. (2005) Mineral assemblages from the vein salband at Săcărimb, Golden Quadrilateral, Romania: I. Sulphides and sulphosalts. Au-Ag-Te-Se deposits, IGCP Project 486. Bulgarian Academy of Sciences; *Geochemistry, Mineralogy and Petrology (Sofia)*, **43**, 47–55.

Engel, P. and Nowacki, W. (1969) Kristallstruktur von Baumhauerit. *Zeitschrift für Kristallographie*, **129**,178–202.

Engel, P. and Nowacki, W. (1970) Die Kristallstruktur von Rathit-II ($As_{25}S_{56}Pb_{65}^{vii}Pb_{12}^{ix}$). *Zeitschrift für Kristallographie*, **131**, 356–375.

Ferraris, G., Makovicky, E. and Merlino, S. (2008) *Crystallography of Modular Materials.* Oxford University Press, Oxford, UK.

Iitaka, Y. and Nowacki, W. (1961) A refinement of the pseudo crystal structure of scleroclase $PbAs_2S_4$. *Acta Crystallographica* **14**, 1291–1292.

Jambor, J.L. (1967*a*) New lead sulfantimonides from Madoc, Ontario – Part 1. *The Canadian Mineralogist*, **9**, 7–24.

Jambor, J.L. (1967*b*) New lead sulfantimonides from Madoc, Ontario. Part 2 – Mineral descriptions. *The Canadian Mineralogist*, **9**, 191–213.

Johan, Z. and Mantienne, J. (2000) Thallium-rich mineralization at Jas Roux, Hautes-Alpes, France: a complex epithermal, sediment-hosted, ore-forming system. *Journal of the Czech Geological Society*, **45**, 63–77.

Khodaparast, M., Tajedin, H. and Shahrokhi, V. (2010) Nature of fluid inclusions of gold mineralization at Barika shear zone: Example of Kuroko type gold mineralization in the west of Iran. *The 1st International Applied Geological Congress, Department of Geology, Islamic Azad University – Mashad Branch, Iran, 26-28 April 2010.*

Kraus, W. and Nolze, G. (1999) *PowderCell 2.3.* Federal Institute for Materials Research and Testing, Berlin.

Le Bihan, M.T. (1962) Etude structurale de quelques sulfures de plomb et d'arsenic naturels du gisement de Binn. *Bulletin de la Société Francaise de Minéralogie et de Cristallographie*, **99**, 351–360.

Makovicky, E. (1985) The building principles and classification of sulphosalts based on the SnS archetype. *Fortschrift für Mineralogie*, **63**, 45–89.

Makovicky, E. and Topa, D. (2012) Twinnite, $Pb_{0.8}Tl_{0.1}Sb_{1.3}As_{0.80}S_4$, the OD character and the question of its polytypism. *Zeitschrift für Kristallographie*, **227**, 468–475.

Makovicky, E. and Topa, D. (2013) The crystal structure of barikaite. *Mineralogical Magazine*, in press.

Makovicky, E., Topa, D., Tajjedin, H., Rastad, E. and Yaghubpur, A. (2012) The crystal structure of guettardite, $PbAsSbS_4$. *The Canadian Mineralogist*, **50**, 253–265.

Mantienne, J. (1974) *La minéralisation metallifère de Jas-Roux (Hautes-Alpes).* Thèse de Doctorat Universitaire, Université de Paris 6, 153 pp.

Marumo, F. and Nowacki, W. (1965) The crystal structure of rathite-I. *Zeitschrift für Kristallographie*, **122**, 433–456.

Marumo, F. and Nowacki, W. (1967) The crystal structure of dufrénoysite, $Pb_{16}As_{16}S_{40}$. *Zeitschrift für Kristallographie*, **124**, 409–419.

Orlandi, P., Biagioni, C., Bonaccorsi, E., Moëlo, Y. and Paar, W.H. (2012) Lead-antimony sulfosalts from Tuscany (Italy). XII. Boscardinite, $TlPb_3(Sb_7As_2)_{\Sigma 9}S_{18}$, a new mineral species from the Monte Arsiccio mine: occurrence and crystal structure. *The Canadian Mineralogist*, **50**, 235–251.

Ozawa, T. and Nowacki, W. (1974) Note on the mineral rathite-IV. *Neues Jahrbuch für Mineralogie Monatshefte*, **1974**, 530–531.

Paar, W.H., Pring, A., Moëlo, Y., Stanley, C.J., Putz, H., Topa, D., Roberts, A.C. and Braithwaite, R.S.W. (2009) Daliranite, $PbHgAs_2S_6$, a new sulfosalt from the Zarshouran Au-As deposit, Takab region, Iran. *Mineralogical Magazine*, **73**, 871–881.

Ribár, B., Nicca, Ch. and Nowacki, W. (1969) Dreidimensionale Verfeinerung der Kristallstruktur von Dufrénoysite, $Pb_8As_8S_{20}$. *Zeitschrift für Kristallographie*, **130**, 15–40.

Topa, D., Makovicky, E., Putz, H., Zagler, G. and Tajeddin, H. (2013*a*) Barikaite, IMA 2012-055. CNMMC Newletter No. 15, February 2013, page 4; *Mineralogical Magazine*, **77**, 1–12.

Topa, D., Makovicky, E., Putz, H., Zagler, G. and Tajeddin, H. (2013*b*) Ferdowsiite, IMA 2012-062. CNMMC Newletter No. 15, February 2013, page 9; *Mineralogical Magazine*, **77**, 1–12.

Topa, D., Makovicky, E., Putz, H., Zagler, G. and Tajeddin, H. (2013*c*) Arsenquatrandorite, IMA 2012-087. CNMNC Newsletter No.16, August 2013, page 2696; *Mineralogical Magazine*, **77**, 2695–2709.